Paper No. 16

ROTORCRAFT COMPUTATIONAL FLUID DYNAMICS
- RECENT DEVELOPMENTS AT MCDONNELL DOUGLAS

R.D. JANAKIRAM - A.A. HASSAN

MCDONNELL DOUGLAS HELICOPTER COMPANY
MESA, AZ, USA

R. AGARWAL

MCDONNELL DOUGLAS RESEARCH LABS
ST. LOUIS, MO, USA

20-23 September, 1988
MILANO, ITALY

ROTORCRAFT COMPUTATIONAL FLUID DYNAMICS
- RECENT DEVELOPMENTS AT MCDONNELL DOUGLAS

R.D. JANAKIRAM - A.A. HASSAN
MCDONNELL DOUGLAS HELICOPTER COMPANY
MESA, AZ, USA

R. AGARWAL
MCDONNELL DOUGLAS RESEARCH LABS
ST. LOUIS, MO, USA

ABSTRACT

Recent developments at McDonnell Douglas in the application, validation and development of computational fluid dynamics (CFD) techniques to solve specific rotor aerodynamics problems are presented. McDonnell Douglas's rotor full-potential flow solver, RFS2, has been validated against a comprehensive set of flight test data. RFS2 was shown to be a reasonably accurate and very efficient tool in modeling nonlinear transonic flows on advancing rotor blades. RFS2 was also modified to model the rotor blade-vortex-interaction aerodynamics, and the predictions compare favorably with test data for subcritical interactions. The McDonnell Douglas rotor Euler flow solver, MDROTH, was shown to provide good results for strong supercritical flows at the expense of significantly increased computer CPU time. The McDonnell Douglas 2-D, full Reynolds averaged Navier-Stokes solver DSS2 was able to predict reasonably well the transonic static and dynamic rotor airfoils characteristics, especially the lift characteristics. Navier- Stokes solvers are being used to model the effects of novel tip configurations (BERP) on retreating blade stall and in the simulation of the flow environment of a circulation control tailboom of the McDonnell Douglas NOTAR helicopter configuration.

NOMENCLATURE

AR	rotor aspect ratio
C	rotor chord
C_D	airfoil sectional drag coefficient
C_L	airfoil sectional lift coefficient
C_M	airfoil sectional moment coefficient
C_T	thrust coefficient
K	reduced frequency of unsteady motion
M_t	tip Mach number
RBAR	nondimensional rotor radius
Re	airfoil chord Reynold number
RV/C	nondimensional vortex core radius
X/C	nondimensional chordwise station
ZV/C	nondimensional vortex miss distance
μ	rotor advance ratio
α	angle of attack
θ	collective pitch angle
σ	rotor solidity
Γ	nondimensional vortex strength
ψ	rotor blade azimuth

1. INTRODUCTION

Rotorcraft aerodynamics is characterized by nonlinear, three-dimensional and often unsteady rotor flow fields, complex vortical wakes and large interactional effects. With the recent emphasis on higher forward speeds and increased maneuver capability (as required in air-to-air combat operations), the effects of unsteady, non-linear transonic flow near advancing rotor blade tips and dynamic stall on the retreating blades need to be modeled and analyzed to determine optimum rotor configurations for performance, vibration and noise levels. In addition, the strong rotor/wake and rotor/body aerodynamic interactions need to be modeled and accounted for accurately in any optimum rotor design. The structural dynamics of rotor blades also plays a significant role in the determination of rotor airloads.

For several years, engineers in the rotorcraft industry have relied on empirical based simple linear aerodynamic theories and wind tunnel data to estimate the airloads on rotors and fuselages. As the flight envelopes of the modern rotorcraft expand, the linear theories in use today are being stretched to the limit and are simply not adequate for blade tip aerodynamic evaluation and rotor noise prediction. Since the underlying aerodynamic phenomena in modern rotorcraft are essentially three-dimensional, unsteady and nonlinear, it is necessary to solve the governing fluid dynamic equations directly for an accurate estimation of rotorcraft flow field. With the advent of large-scale super computers, it is now possible to solve these equations using finite-difference techniques in a relatively cost effective manner. Computational fluid dynamics (CFD) techniques have emerged in the past decade and are used widely in the fixed-wing industry at present to estimate flow fields about the complete aircraft and to design components such as wings, engine inlets, etc.

Success in the fixed-wing industry and rapid advances in cost effective computing capability have spurred some engineers and scientists in the rotorcraft industry and government labs to modify a few mature CFD techniques originally developed for fixed wing applications, for rotorcraft applications. Early work involved the development of quasi-steady full-potential, and unsteady small-disturbance potential flow solvers [1,2] to model the nonlinear transonic aerodynamics of advancing rotor blades. Though these solvers have had limited success, they prompted the development of more accurate unsteady full-potential flow solvers [3,4,5] for high-speed rotor flow computations. These solvers are based on the solutions to the 3-D, unsteady, full-potential flow equation in conjunction with Bernoulli's equation. They typically use finite-difference techniques on a body-conforming computational grid surrounding a portion of the rotor blades. The near wake effects are included through a jump in the velocity potential across the wake cut. These solvers require input of integral wake code solutions to provide the effects of induced inflow due to the far wake.

It was shown [6] that it is practical to combine finite-difference computations with existing integral aerodynamics and loads trim codes, and that the conservative full-potential codes [3,4] offer the best combination of speed and accuracy. Potential flow solvers are well known for their reasonably accurate results for flows with weak shocks.

However, they depend on a separate integral wake code to provide vortex-induced flow effects, and their accuracy is therefore limited by these wake codes. Steinhoff and Ramachandran [7] have recently developed a method which simultaneously computes the transonic aerodynamic flow field and the vortex wake development for rotor blades in steady state hover. This analysis uses a full-potential flow solution with a vortex embedding method.

The inherent irrotationality and inviscid flow assumptions of the potential flow solvers limit their applicability. In flows where strong shocks and viscous effects are present, it is necessary to solve the more accurate Euler equations which permit vortical flows and Navier-Stokes equations which permit modeling of viscous effects. In the past few years several Euler and Navier-Stokes flow solvers were developed for rotorcraft applications. These solvers require an order of magnitude more of computer resources (memory and speed) than those required for full-potential flow solvers, and therefore are mainly being implemented in a research mode. Euler solvers have been developed [8,9,10] to capture the near vortex wakes and to provide transonic flow effects on multi-bladed rotors in steady state hover flight conditions, and the results are promising. Other Euler solvers which use prescribed vortex-induced inflow obtained from separate integral wake code results are reported in Refs. [11,12]. Some of the published Euler results show good correlations, and as with the potential flow solvers, it appears that the accuracy of the vortex-induced inflow predictions is a strong limiting factor.

In recent years, full Reynolds-averaged and thin/slender-layer forms of Reynolds-averaged Navier-Stokes solvers have been developed for rotorcraft applications. In most instances these are natural extensions to existing Euler solvers, and they often include an algebraic turbulence model. Early applications of these solvers [13,14] included the prediction of static rotor airfoil characteristics and unsteady airfoil-vortex interactions. It was shown that these codes are capable of predicting the transonic airfoil characteristics as accurate as wind tunnel measurements. Navier-Stokes solvers for rotor flow predictions are relatively new [15,16], and preliminary results for the flow prediction of a hovering rotor blade are encouraging. Two recently published papers [17,18] provide an overview of some of the Euler and Navier-Stokes solvers developed for rotorcraft applications.

Recently, spurred by the need to determine detailed rotor blade airloads for use in aeracoustic predictions and to determine the effect of novel tip shapes on rotor performance and acoustics, a series of CFD codes for rotorcraft applications were developed at McDonnell Douglas. An unsteady, 3-D, rotor full-potential flow solver designated RFS2, and full Reynolds-averaged Navier-Stokes solvers DSS2 (2-D) and DSS3 (quasi-3D) were developed by Dr. L.N. Sankar under the sponsorship of McDonnell Douglas Helicopter Company. A 3-D rotor Euler solver (MDROTH) and a thin-layer Reynolds-averaged Navier-Stokes solver for rotor flows were developed at McDonnell Douglas Research Labs. The details regarding the formulations used, and validation studies conducted with these CFD codes were reported in Refs. [3,12,16,18].

In this paper, some recent developments at McDonnell Douglas for analyzing the rotor flow field using full-potential, Euler, and Navier-Stokes solvers will be discussed. Specifically, the developments at McDonnell Douglas Helicopter Company (MDHC) include: more comprehensive validation studies with the rotor full potential flow solver, RFS2, and its application to the prediction of three-dimensional rotor blade-vortex-interaction (BVI) aerodynamics; recent modifications to RFS2 to improve its accuracy and modeling capabilities; and the application of the two-dimensional Navier-Stokes solver, DSS2, to predict the static and dynamic stall characteristics of one of the new generation MDHC airfoils. The developments at McDonnell Douglas Research Labs include more recent validation studies of its rotor Euler and Navier-Stokes solvers. Some MDHC plans will be addressed regarding the use of these CFD techniques for the prediction of the lifting characteristics of blades with novel tip shapes (BERP-like tips), numerical simulation of circulation control flow-fields around the tail boom, and rotor performance predictions of the McDonnell Douglas NOTAR helicopter configuration.

2. POTENTIAL FLOW SOLVER

In 1985, Dr. Sankar of Georgia Institute of Technology, under sponsorship from McDonnell Douglas Helicopter Company, developed a rotor full-potential flow solver, designated RFS2 [3]. RFS2 provides solutions to the three-dimensional, unsteady compressible full-potential equation in conservation form on a body-fitted coordinate system using a Strongly Implicit Procedure (SIP). The use of a Strongly Implicit Procedure (SIP) allows the solver to handle both the quasi-steady and the unsteady rotor flow field calculations using the same numerical algorithm. Rotor wake, blade motion and trim effects are provided as input to RFS2 from a separate integral wake code. In the original version of RFS2 designated RFS2H, wake and blade motion effects are modeled as corrections to section angles of attack at several blade radial stations. A C-type grid topology is used in this solver. Some of the special features of the solver include consistent metric differencing and monotonic density biasing. A more complete description of the solver and some comparisons of predictions with experimental data were reported earlier [3,6,18]. It has been demonstrated that RFS2 is perhaps the most efficient solver among the currently available rotor full-potential flow solvers, requiring the least amount of computer CPU time while providing generally accurate solutions [6].

Over the past year, MDHC with assistance from Dr. Sankar of Georgia Institute of Technology, has embarked on a comprehensive investigation of RFS2 to determine its accuracy through further validation studies and to improve its capability to model such features as rotor blade-vortex interactions, blade motion effects and viscous flow effects. Some of the results of this study are described here.

2.1 Validation of RFS2. The original RFS2 version (RFS2H), where rotor wake and blade motion effects are modeled in the form of corrections to section angles of attack, was exercised to predict the flow fields for two transonic flow cases for which experimental data was available. These cases correspond to two flight test conditions for the Aerospatiale Gazelle helicopter [19]. In these tests, pressure measurements

were recorded at three outboard main rotor blade radial stations. RFS2 predictions are compared here with the test data at representative azimuthal stations covering the complete rotor revolution. The CAMRAD (wake and trim) code [20] was used to provide the angle of attack input to RFS2 for both of these test conditions. A partial inflow routine which removes the effect of the near blade wake (accounted for in RFS2) from the CAMRAD wake computations over the complete rotor revolution was recently developed at U.S. Army Aeroflightdynamics Directorate (AFDD) and was made available to MDHC. Iterations were also performed between the CAMRAD and RFS2 solvers to match the lift coefficients. The iterative procedure used is identical to that reported in Ref. [21] where similar comparisons were made using the full-potential flow solver, FPR, developed by U.S. Army's AFDD [21]. Here, correlations are made between RFS2 predictions and the test data at the same radial and azimuthal stations reported in Ref. [21].

Figure (1) illustrates results from RFS2 predictions and the flight tests for the Gazelle main rotor at an advance ratio of 0.378, a hover tip Mach number of 0.63 and a C_T/σ of 0.0645. Predictions were made with a mesh size of 121x24x12 (91x19 points on the blade surface). The computations took about 312 secs on a CRAY X-MP to perform a complete unsteady calculation covering a full rotor revolution. Predictions shown in Fig. (1) correspond to the results following two iterations between RFS2 and the trim code CAMRAD. It can be seen from Fig. (1) that the correlations between the predictions and test data are good for most of the radial and azimuthal stations considered. Shock locations and strengths are predicted reasonably well at the advancing blade azimuthal stations. However, the correlations for the lower surface pressures could be further improved, perhaps with the inclusion of nonisentropic flow effects and viscous flow effects. At the retreating blade azimuthal stations (Fig. (1)) the leading edge suction peaks are well predicted, although the correlation at the aft chordwise stations is not as good. This could be improved by incorporating viscous flow effects. The small differences seen between the upper and lower surface pressure values at the blade's trailing edge are due to the relatively coarse grid resolution associated with the sheared parabolic grid. It is seen later (in RFS2 predictions for a blade-vortex-interaction case) that the use of a grid providing higher resolution near the trailing edge (cosine distribution) removes this anomaly. It should be noted that the RFS2 predictions shown in Fig. (1) are only as good as the angles of attack predictions provided by CAMRAD and that some of the discrepancies between the predictions and test data can be attributed to inaccurate CAMRAD predictions. In the trim code CAMRAD, a rigid wake model was used.

Figure (2) illustrates comparisons between RFS2 predictions and flight test data for the Gazelle main rotor at an advance ratio of 0.344, a hover tip Mach number of 0.63 and a C_T/σ of 0.0649. The correlation at advancing blade azimuthal stations is generally good except at the azimuthal station of 120 deg and radial station of 0.75. Similar results were also reported in Ref. [22]. On the retreating side, the correlations between the predictions and test data is mixed. This poor correlation can be attributed partially to the inaccurate angles of attack computed in CAMRAD and provided to RFS2 as input. The rigid wake model used may not be adequate at this advance ratio. Also, at the azimuthal station of 180 deg, some of the poor correlation can be attributed to the absence of accounting for the fuselage induced upwash effects in CAMRAD.

The poor correlation observed at the azimuthal station of 300 deg could be due to inaccurate estimation of wake induced velocities in CAMRAD as well as the lack of modeling of viscous flow effects in RFS2. Generally for both test cases described above, RFS2 predictions are in agreement with those reported in Ref. [21]. However, it should be noted that these predictions require only ten minutes of CRAY X-MP time (for two iterations of RFS2) for a complete rotor revolution.

The correlation study of RFS2 (RFS2H) described above revealed that the correlation with test data can be further improved if modeling of viscous flow effects is included. It was also felt that the rotor blade motions and vortex-induced inflow should be accounted for in a more accurate fashion than the angle of attack approach currently used. Therefore, as reported in Ref. [22], several improvements have been made to RFS2 to allow for more accurate and flexible analysis of helicopter rotor blade flow fields. These modifications include; a more explicit treatment of rotor blade motion and vortex wake-induced inflow, use of a steady 2-D integral boundary layer analysis utilizing strip theory for viscous flow effects, and a Newton iteration method to reduce the number of global time steps and therefore the total CPU time required for a given analysis. These modifications are described in detail in Ref. [23]. The new version of RFS2 with those modifications has been designated RFS2L. The correlation between RFS2L predictions and experimental data, as reported in Ref. [23], is less than satisfactory. A comprehensive investigation of RFS2L is underway to identify the effects of each of these new modifications. It is believed that once fully validated, RFS2L will be a very efficient, accurate rotor full-potential flow solver which can be used routinely in the aerodynamic design and analysis of rotors.

2.2 MODELING OF THREE-DIMENSIONAL ROTOR BLADE-VORTEX INTERACTIONS (BVI):

Since RFS2 is based on a potential formulation, it does not admit distributed vortices in the flow field except, of course, along well defined coordinate cuts such as the trailing edge wake where the jump in the potential represents the bound vortex strength. Embedded vortex wakes have been modeled in full potential flow solvers [23,24] using what is commonly referred to as "branch cut methods". These methods, despite their accuracy, are well suited for modeling geometrically simple wake elements on rigid grids. For curved wake elements, an adaptive grid becomes a must to avoid the cumbersome effort necessary to interpolate the wake position and induced velocities at the neighboring grid points. As a result, the implementation of these methods to model blade-vortex interactions (BVI) has been limited to two-dimensional flows [23,25]. Here, we examine two alternative approaches for the BVI problem which have proved to be efficient and, to some extent, equally easy to adapt to the two and three-dimensional flow problems. These approaches have been implemented in the RFS2 solver and at present are being validated for their relative accuracy and robustness.

Split potential "or perturbation" method ; this approach was first suggested by Steinhoff [26] and has been successfully applied for modeling two and three-dimensional BVI using full potential [23,27], and Navier-Stokes formulations [14]. Here, the velocity potential function, or any of the dependent flow variables for higher-order models, are decomposed into two parts; the first representing the perturbation solely

due to the vortex element, and the second representing the potential or the variation in the dependent flow variables resulting from the flow past the blade and its wake shed vorticity.

Surface "or transpiration velocity" method ; this method is by far the simplest to implement in any two or three-dimensional flow solver. In this method, vortex-induced velocities are computed at all grid locations on the surface of the blade using Biot-Savart law. Once these velocities are computed, the zero normal velocity boundary condition is modified such that the relative velocity between the solid and the fluid is zero.

As mentioned earlier, the RFS2 solver in its present form is capable of modeling three-dimensional BVI using the perturbation and surface approaches. However, due to the simplicity of the latter approach and its small CPU time requirements (5 CPU minutes on a CRAY X-MP for a 0 - 360 unsteady computation), the surface method was used to modify the solver. The modified solver was then coupled with the comprehensive rotor trim solver CAMRAD [20] to model BVI resulting from the interaction between the rotor and finite length element(s) of its own generated wake during low-speed descent flight conditions. Further details on this general interaction will be discussed in an upcoming paper.

To validate the modified version of the solver, simulations of the three-dimensional BVI experiments of Caradonna, Laub, and Tung [28] and more recently of Caradonna, Lautenschlager, and Silva [29] were performed. In their experiment, the interaction was simulated by means of a rotating untwisted rectangular blade (having a NACA0012 section, aspect ratio of 7) interacting with a vortex which was generated at the tip of a fixed wing located upstream of the blade. A sketch illustrating the experimental setup is depicted in Fig. (3). In Figs. (4a,4b) a comparison between the predicted and measured upper surface pressures at 2% chord during a parallel BVI is illustrated. In this example, the vortex is aligned with the 0 - 180 deg. azimuth and is located at 0.25 C (Fig. (4a)), and 0.40 C (Fig. (4b)) above the blade's upper surface. The vortex strength reported in Ref.[29], a finite vortex core radius of 0.225 C, and Scully's [30] vortex core model for computing the vortex-induced velocities both used. Numerical experimentation with other core models have indicated that Scully's vortex model (distributed vorticity) provides a more realistic velocity distribution as compared to the concentrated vorticity core model. The correlation for the miss distance of 0.25C (Fig. (4a)) is very good, however, for a miss distance of 0.4C, the solver tends to overpredict the surface pressures. Figure (5) illustrates the effect of varying the vortex strength on the computed surface pressures for the conditions of Fig. (4b). As seen, an improvement in the correlation with the experimental data is obtained when the vortex strength is reduced by 10%. It is conjectured that as the vortex passes above the blade it experiences a rapid change in the axial velocity due to the pressure field of the blade, hence reducing the miss distance and consequently increasing the vortex-induced velocities computed on the blade's surface. A second factor not accounted for in the present model is the actual distortion and resulting dissipation of the vortex during and after its close encounter with a blade.

In order to determine the ability of RFS2 to predict the entire chordwise pressure distributions during parallel BVI, comparisons are made between the predicted surface pressures and the experimental data of Ref. [28]. It should be noted that the experimental data is from an earlier experiment by Caradonna et al. [28], and therefore, some of the BVI parameters are different from those described above. Figure (6a) illustrates a comparison between the test data and the predicted surface pressures using the subcritical BVI parameters reported in Ref. [28]. The correlation is very good for the lower surface (vortex side) but is not as good for the upper surface. As seen in Fig. (6b), the correlation for the upper surface can be slightly improved if the vortex strength is reduced by 25%. For the same interaction conditions of Fig. (6a), the variations of the predicted sectional lift and moment coefficients as a function of blade azimuth are illustrated in Fig. (7). These predictions clearly show the impulsive effects of the parallel BVI on the computed loads as the blade approaches the interaction azimuth of 180 deg.

Plans are underway to use the modified RFS2 solver for predicting supercritical BVI conditions in the near future. The plans also include conducting a parallel validation study using the split-potential approach to model parallel BVI. Both approaches will be used to model the near parallel BVI which occur on rotors in the descent flight condition. It should be noted that the transpiration velocity approach is very efficient however, its accuracy in modeling subcritical and supercritical BVI remains to be established more clearly. This effort will be pursued in the near future.

3. EULER FLOW SOLVER

In recent years an Euler/Navier-Stokes solver designated MDROTH was developed at McDonnell Douglas Research Laboratories (MDRL) to predict the transonic flow-field of a rotor in hover and forward flight. The code solves the three-dimensional strongly conservative forms of the Euler/Navier-Stokes equations in a rotating coordinate system on a body conforming O-type grid surrounding the rotor blade. The equations are recast in absolute-flow variables so that the absolute flow in the far field in uniform but the relative flow is nonuniform. The equations are solved for the absolute-flow variables by employing Jameson's finite-volume explicit Runge-Kutta time-stepping scheme [31]. The details of the methodology used and a set of comparisons between predictions made by the Euler solver, MDROTH and test data were reported in Ref. [14]. Similar to MDHC's full-potential model, rotor blade motion, trim and far wake-induced inflow effects are provided as input to MDROTH in the form of an angle-of-attack distribution along the blade for each blade azimuth. MDROTH has been fully vectorized for optimum performance on a single processor CRAY X-MP and CRAY2. It has also been microtasked on a four-processor CRAY X-MP/48 to reduce the wall clock time by judicious use of various CRAY software techniques [12].

The Euler solver, MDROTH, was exercised to predict the transonic flow field on the advancing blade of a French ONERA three-bladed rotor for which wind tunnel test data (blade surface pressures) is available. The test case selected was a high transonic one with an advance ratio of 0.387 and a hover tip Mach number of 0.63. Here, CAMRAD [20] was used to

provide the angle-of-attack distributions at different blade azimuthal and radial stations. The partial inflow routine within CAMRAD was also used here. Figure (8a) illustrates comparisons between MDROTH predictions and the wind tunnel test data. These predictions correspond to a partial trim since no iterations were performed between MDROTH and CAMRAD to match the blade lift coefficients. However, it was shown that for this case there is very little difference between the partial and full trim [6] results. MDROTH predictions were made with a mesh size of 97x33x33. For comparison purposes the same calculations were also performed with the full-potential flow solver RFS2 (mesh size 121x24x12) and compared with the test data (Fig. (8b)). In Fig. (8b) the RFS2 (RFS2H) calculations correspond to full trim (i.e., 2 passes through RFS2). As expected, it can be easily seen that the Euler solver was able to predict the location and strength of the shock more accurately than the full-potential flow solver at the blade azimuths of 90, 120 and 150 deg. MDROTH was also able to predict lower surface pressures accurately. Some of the discrepancies between the predicted and measured leading edge suction peaks could be due to an inaccurate input of angles-of-attack provided by CAMRAD. At the blade azimuth of 60 deg, there was not any significant difference between MDROTH and RFS2 predictions. These results indicate that it may be necessary to use the Euler solver for strong supercritical rotor flows due to the presence of relatively strong shocks. However, it should be noted that the Euler computations reported here require about 8 hours of CPU time on a CRAY X-MP. Therefore, unless dramatic improvements are made to reduce the computer CPU requirements of these solvers, they may only be used in the research mode.

A fixed wing version of the Euler code MDROTH was recently used at MDRL to determine the effects of a close interaction between an upstream generated vortex and a wing. The velocity perturbation approach defined earlier was used. This is similar to the split potential approach used in full-potential flow solvers in modeling BVI [24]. For a given velocity field due to the vortex, Euler equations are solved for the perturbation velocity which is the difference between the total velocity and the vortex induced velocity. Figure (9) is a schematic of the wing/vortex interaction configuration which was simulated numerically using the Euler solver. Figure (10) illustrates a comparison between the predicted and measured spanwise lift distribution during blade-vortex interaction in a supersonic onset flow. As seen, the correlation is good except very near the wall. A surface transpiration velocity approach was also used, but the correlation was not quite as good except at the spanwise stations close to the vortex.

4. NAVIER-STOKES FLOW SOLVERS

It is well known that two phenomena having great impact on rotor performance at high speeds are retreating blade stall and compressibility effects on the advancing blades. A robust numerical solution procedure for analyzing the rotor flow environment must therefore be capable of predicting accurately the inherent unsteadiness of the flow, compressibility effects, and be suitable for analyzing flows with regions of massive separation. The solutions of the unsteady compressible Navier-Stokes equations offer the potential for modeling the physics of all these flow features. However, aside from certain uncertainties

associated with turbulence modeling, imposed approximations to these equations tend to limit their range of applicability for certain problems of interest. For example, solvers which are based on the solutions to the thin-layer Reynolds-averaged Navier-Stokes equations, such as ARC2D [13], are limited to analyzing flows at small to moderate angles-of-attack. Their usefulness in the prediction of sectional loads at stall and post stall angles-of-attack is hindered by the limitations imposed by the formulation employed. Here we describe some of the recent advances in the simulation of the airfoil and the rotor flow environments using Navier-Stokes based formulations.

Under a cooperative research program between Georgia Institute of Technology and McDonnell Douglas Helicopter Company, two dynamic stall solvers were developed. The first, designated DSS2, solves the dynamic stall problem for two-dimensional flows. The second solver designated DSS3, solves the dynamic stall problem for quasi-three-dimensional flows. The solvers are based on the solutions to the two and quasi-three-dimensional unsteady, compressible, full Reynolds-averaged Navier-Stokes equations on a body-fitted C-type grid. For unsteady computations, the grid is allowed to undergo pitching or plunging motion following the prescribed oscillatory motion of the airfoil. A modified Baldwin-Lomax [32] two-layer algebraic eddy viscosity model is incorporated in the formulation to model turbulent shear stresses. The steady and unsteady results presented here represent those obtained using the DSS2 solver. For additional results illustrating the capabilities of the DSS3 solver, the reader is referred to Ref. [18].

In Figs. (11a-c) comparisons are made between the predicted steady lift, drag, and moment coefficients and the available experimental data for the NACA0012 airfoil at a subcritical Mach number of 0.3 and a chord Reynolds number of 3.91 million. As seen, a considerable improvement in the correlation with the data is obtained when assuming a fully turbulent flow past the airfoil. In Fig. (11d), comparisons are made between the predicted and measured steady lift characteristics for the McDonnell Douglas HH-06 airfoil. The results clearly indicate the accuracy of the solver in the prediction of sectional lift variation at and beyond the maximum stall angle. However, despite this very good agreement in the predicted lift coefficients, it was found out that the predicted moment and drag coefficients for the HH-06 airfoil were respectively 24% and 33% lower than those measured for low angles of attack, and on the order of 3% and 36% higher than those measured for angles of attack exceeding the static stall angle. This discrepancy is at present being attributed primarily to the relatively coarse mesh utilized in the computation (157x58 with 97 grid points on the surface of the airfoil) and to a number of uncertainties in the turbulence model.

Figure (12a) depicts the variation of the predicted sectional drag coefficient at zero-lift conditions as a function of free stream Mach number for the NACA0012 airfoil. Fig. (12b) illustrates the relative accuracy of the solver in predicting $dC_L/d\alpha$ at various free stream Mach numbers for a nonlifting NACA0012 airfoil. As seen, all points representing the predicted values fall within or on the band representing the available experimental data. Figure (13) illustrates the predicted unsteady lift, drag, and moment coefficients for the NACA0012 airfoil while undergoing pitch oscillations about the quarter chord point. Here,

the airfoil oscillates about a mean angle of 15 deg with an amplitude of 10 deg and a reduced frequency of 0.158 which is typical to those of a retreating blade. For the unsteady lift computation, good correlation with the experimental data is observed over most of the cycle. However, discrepancies are noticed in the predicted unsteady drag and moments as the airfoil reaches the maximum angle of 25 deg during the upstroke portion of the cycle and also as it starts the downstroke pitching motion. This discrepancy is attributed to the use of the simple Baldwin-Lomax turbulence model and does not seem to be grid dependent.

It is noteworthy to mention that in addition to utilizing the DSS2 solver in the prediction of steady and unsteady airfoil characteristics for the rotor dynamic and aerodynamic applications, modifications are being made on the solver to model a problem of particular interest to McDonnell Douglas Helicopters. The problem constitutes analyzing the flow past the circulation control tail boom of a NOTAR helicopter configuration, Fig. (14). The NOTAR concept uses a circulation control tail boom where low velocity jets are tangentially blown through appropriately located slots on the circumference of the nearly circular section of the tail boom. These low velocity jets in combination with the rotor wake flow impinging on the boom for a hover flight condition, will generate a lateral force on the tail boom which will provide part of the required antitorque force (about 60%) for the hover condition. As a first step towards modeling the actual three-dimensional flow problem, a number of assumptions to simplify the analysis have been made. They include uniform onset flow and two-dimensional flow at every station along the tail boom (i.e., strip theory is assumed), see Fig. (15). The modifications to the solver entail altering the surface boundary conditions to model the surface jets at specific points along the circumference, and the incorporation of the more comprehensive two-equation $K-\epsilon$ turbulence model. This turbulence model is more suitable for this problem since the current C-grid mesh cut causes a misalignment of the resulting wake when connecting the cylinder to the outflow boundary. At the present time, the grid generation program GRAPE [33] is used to generate a suitable grid to perform the computations.

McDonnell Douglas Research Labs has recently developed a thin-layer Reynolds-averaged Navier-Stokes version of its Euler flow solver MDROTH to compute the rotor flow field [16]. A Baldwin-Lomax algebraic eddy viscosity model is used to model the effects of turbulence. This code was used to predict the surface pressure distributions of a lifting rotor in hover and the results were reported in Ref. [16]. Figure (16) shows a typical correlation between the predictions and test data. An empirical angle-of-attack correction was employed in these calculations to account for the wake effects. It is believed that while the correlation shown in Fig. (16) is satisfactory, it can be substantially improved by using an accurate wake model which excludes the effects of the near wake.

MDHC has recently acquired the 3-D, full Reynolds-averaged compressible, Navier-Stokes solver developed for rotor applications at Georgia Institute of Technology [15]. In this code, the governing equations are solved on an unsteady grid using the Beam-Warming algorithm. The influence of the rotor wake is modeled using the transpiration-velocity technique explained earlier. The code was successfully used in the prediction of blade surface pressures for unsteady nonlifting rotor and steady lifting rotor flow fields [15]. A slightly modified version of the code which is suitable for

modeling high angle-of-attack flows more accurately is currently being used at MDHC to model the effects of novel tip configurations (BERP or BERP-like) on the retreating blade stall of advanced rotors. Despite the large CPU and memory requirements, Navier-Stokes flow solvers are the only means available to numerically simulate a specific class of problems of particular interest to rotor aerodynamicists. They include modeling of massive separated flows on rotorcraft fuselages, dynamic stall on retreating rotor blades in high speed forward flight, and the simulation of the flow environment around the circulation control tail boom of a McDonnell Douglas NOTAR helicopter. Hopefully with further improvements in turbulence modeling and computer architecture (use of large number of parallel processors), Navier-Stokes flow simulations will complement and perhaps reduce the amount of wind tunnel testing required in the development of rotorcraft.

5. CONCLUDING REMARKS

CFD techniques are increasingly being used to solve specific rotor aerodynamic problems such as the nonlinear transonic flows on advancing rotor blades, rotor blade-vortex-interaction and the determination of static, and dynamic stall rotor airfoil characteristics. McDonnell Douglas is currently addressing each of these problems with a variety of CFD techniques ranging from those based on the full-potential flow equation to those based on Euler and Navier-Stokes equations. Based on our recent efforts in these areas, the following conclusions are made:

1.   The rotor full-potential flow solver, RFS2, is a robust code and can be used to model transonic flows on advancing rotor blades. Correlation studies conducted for two sets of transonic cases for which flight test data is available showed that RFS2 can predict blade surface pressures with reasonable accuracy. Some of the discrepancies noted could be due to the lack of viscous flow modeling and an inaccurate estimation of blade angles of attack distributions provided as input to RFS2 from a separate trim/wake code.

2.   RFS2 can be easily modified to model the effects of close rotor blade- vortex interactions. The surface velocity approach is very efficient and has provided reasonably good results for the subcritical blade vortex-interaction problem considered.

3.   As expected, rotor Euler flow solvers provide good results for strong supercritical flows at the expense of significantly increased computational requirements. However, as long as these solvers depend on a separate trim/wake code calculation to provide the angle-of-attack input, their use will be limited.

4.   Navier-Stokes solvers are more attractive than Euler solvers because their ability to accurately model separated flows on the retreating rotor blades and to predict the static and dynamic rotor airfoil characteristics. MDHC's 2-D Navier-Stokes solver, DSS2, has shown some success in predicting the static and dynamic stall characteristics of rotor blade airfoils.

5. Navier-Stokes solvers, despite their requirement for large computer resources, are the only means available to numerically simulate problems such as the effects of novel tip (BERP or BERP-like) configurations on rotor retreating blade stall and provide the details of the flow field about the NOTAR circulation control tail boom.

ACKNOWLEDGEMENTS

REFERENCES

1. Arieli, R., and Tauber, M.E., "Computation of Subsonic and Transonic Flow About Lifting Rotor Blades," AIAA Paper 79-1667, Aug. 1979.

2. Caradonna, F.X., Desopper, A., and Tung, C., "Finite Difference Modeling of Rotor Flows Including Wake Effects," Journal of the American Helicopter Society, Vol. 29, No. 2, Apr. 1984.

3. Sankar, L.N., and Prichard, D.S., "Solution of Transonic Flow Past Rotor Blades Using the Conservative Full Potential Equation," AIAA Paper 85-5012, Oct. 1985.

4. Strawn, R.C., and Caradonna, F.X., "Numerical Modeling of Rotor Flows with a Conservative Form of the Full Potential Equations," AIAA 24th Aerospace Sciences Meeting, Reno, Nev., Jan. 1986.

5. Chang, I.C., "Transonic Flow Analysis for Rotors. Part II: Three-Dimensional Unsteady Full Potential Calculation," NASA TP-2375, Jan. 1985.

6. Caradonna, F.X., and Tung, C., "A Review of Current Finite Difference Rotor Flow Methods," Paper presented at the 42nd Annual Forum of the American Helicopter Society, June 1986.

7. Steinhoff, J., and Ramachandran, K., "A Vortex Embedding Method of Free Wake Analysis of Helicopter Rotor Blades in Hover," Paper presented at the Thirteenth European Rotorcraft Forum, Sept. 1987, Arles, France.

8. Roberts, T.W., and Murman, E.M., "Solution Method for a Hovering Helicopter Using the Euler Equations," AIAA Paper 85-0436, 1985.

9. Kramer, E., Hertel, J., and Wagner, S., "Computation of Subsonic and Transonic Helicopter Rotor Flow Using Euler Equations," Paper No. 14, Thirteenth European Rotorcraft Forum, Sept. 1987, Arles, France.

10. Chen, C.L., McCroskey, W.J., and Ying, S.X., "Euler Solution of Multiblade Rotor Flow," Paper presented at the Thirteenth Rotorcraft Forum, Sept. 1987, Arles, France.

11. Sankar, L.N., and Tung, C., "Euler Calculations for Rotor Configurations in Unsteady Forward Flight," Paper presented at the 42nd Annual Forum of the American Helicopter Society, June 1986.

12. Agarwal, R.K., and Deese, J.E., "An Euler Solver for Calculating the Flow Field of a Helicopter Rotor in Hover and Forward Flight," AIAA Paper 87-1427, June 1987.

13. McCroskey, W.J., Baeder, J.D., and Bridgeman, J.O., "Calculation of Helicopter Airfoil Characteristics for High Tip-Speed Applications," Journal of the American Helicopter Society, Vol. 31, (2), Apr. 1986.

14. Srinivasan, G.R., and McCroskey, W.J., "Numerical Simulations of Airfoil- Vortex Interactions," Vertica, Vol. 11 (1/2), Jan. 1987.

15. Wake, B.E., and Sankar, L.N., "Solutions of the Navier-Stokes Equations for the Flow About a Rotor Blade," Paper presented at the National Specialists Meeting on Aerodynamics and Aeroacoustics, Arlington, Texas, Feb. 1987.

16. Agarwal, R.K., and Deese, J.E., "Navier-Stokes Calculations of the Flow-field of a Helicopter Rotor in Hover," AIAA Paper 88-0106, AIAA 26th Aerospace Sciences Meeting, Reno, Nev., Jan. 1988.

17. McCroskey, W.J., "Some Rotorcraft Applications of Computational Fluid Dynamics," Paper presented at the Second International Conference on Basic Rotorcraft Research, College Park, Maryland, Feb. 1988.

18. JanakiRam, R.D., Hassan, A.A., Charles, B., and Sankar, L.N., "Emerging Role of First-Principles Based Computational Aerodynamics for Rotorcraft Applications," Paper presented at the Second International Conference on Basic Rotorcraft Research, College Park, Maryland, Feb. 1988.

19. Yamauchi, G.K., Heffernan, R.M., and Gaubert, M., "Correlation of SA349/2 Helicopter Flight Test Data with a Comprehensive Rotorcraft Model," Paper No. 74, Presented at the Twelfth European Rotorcraft Forum, Sept. 1986, Garmisch-Partenkirchen, F.R.G.

20. Johnson, W., "A Comprehensive Analytical Model of Rotorcraft Aerodynamics and Dynamics. Part I, Analysis Development," NASA TM-81182, 1980.

21. Strawn, C., and Tung, C., "Predictions of Unsteady Transonic Rotor Loads with a Full-Potential Rotor Code," Paper presented at the 43rd Annual Forum of the American Helicopter Society, May, 1987.

22. Prichard, D.S., and Sankar, L.N., "Improvements to Transonic Flowfield Calculations," Paper presented at the 44th Annual Forum of the American Helicopter Society, June, 1988.

23. Jones, H. E. "Full Potential Modeling of Blade-Vortex Interactions," Ph.D Dissertation, The George Washington University, February 1987.

24. Egolf, T. A. and Sparks, S. P. "A Full Potential Rotor Analysis With Wake Influence Using an Inner-Outer Domain Technique," Journal of the American Helicopter Society, Vol. 32, No. 3, July 1987.

25. George, A. R. and Lyrintzis, A. S. "Mid-Field and Far-Field Calculations of Blade-Vortex Interactions," AIAA Paper No. 86-1854, 1986.

26. Steinhoff, J. and Suryanarayanan, K. "The Treatment of Vortex Sheets in Compressible Potential Flow," Proceedings of the AIAA Symposium on Computational Fluid Dynamics, July 1983.

27.   Strawn, R. C. and Tung, C. "The Prediction of Transonic Loading On Advancing Helicopter Rotors," AGARD/FDP Symposium on Applications of Computational Fluid Dynamics in Aeronautics, Aix-en-Provence, France, April 1986.

28.   Caradonna, F. X., Laub, G. H. and Tung, C. "An Experimental Investigation of the Parallel Blade-Vortex Interaction," NASA TM-86005, October 1984.

29.   Caradonna, F. X., Lautenschlager, J. L. and Silva, M. J. "An Experimental Study of Rotor-Vortex Interactions," AIAA Paper No. 88-0045, 1988.

30.   Johnson, W. "Helicopter Theory," Princeton University Press, 1980.

31.   Jameson, A., Schmidt, W., and Turkel, E., "Numerical Solution of the Euler Equations by Finite Volume Methods Using Runge-Kutta Time-Stepping Schemes," AIAA Paper 81-1259, 1981.

32.   Baldwin, B.S., and Lomax, H., "Thin-Layer Approximation and Algebraic Model for Separated Turbulent Flows," AIAA Paper 78-257, 1978.

33.   Sorenson, R.L., "A Computer Program to Generate Two-Dimensional Grids About Airfoils and Other Shapes by the Use of Poisson's Equations," NASA TM 81198, May 1980.
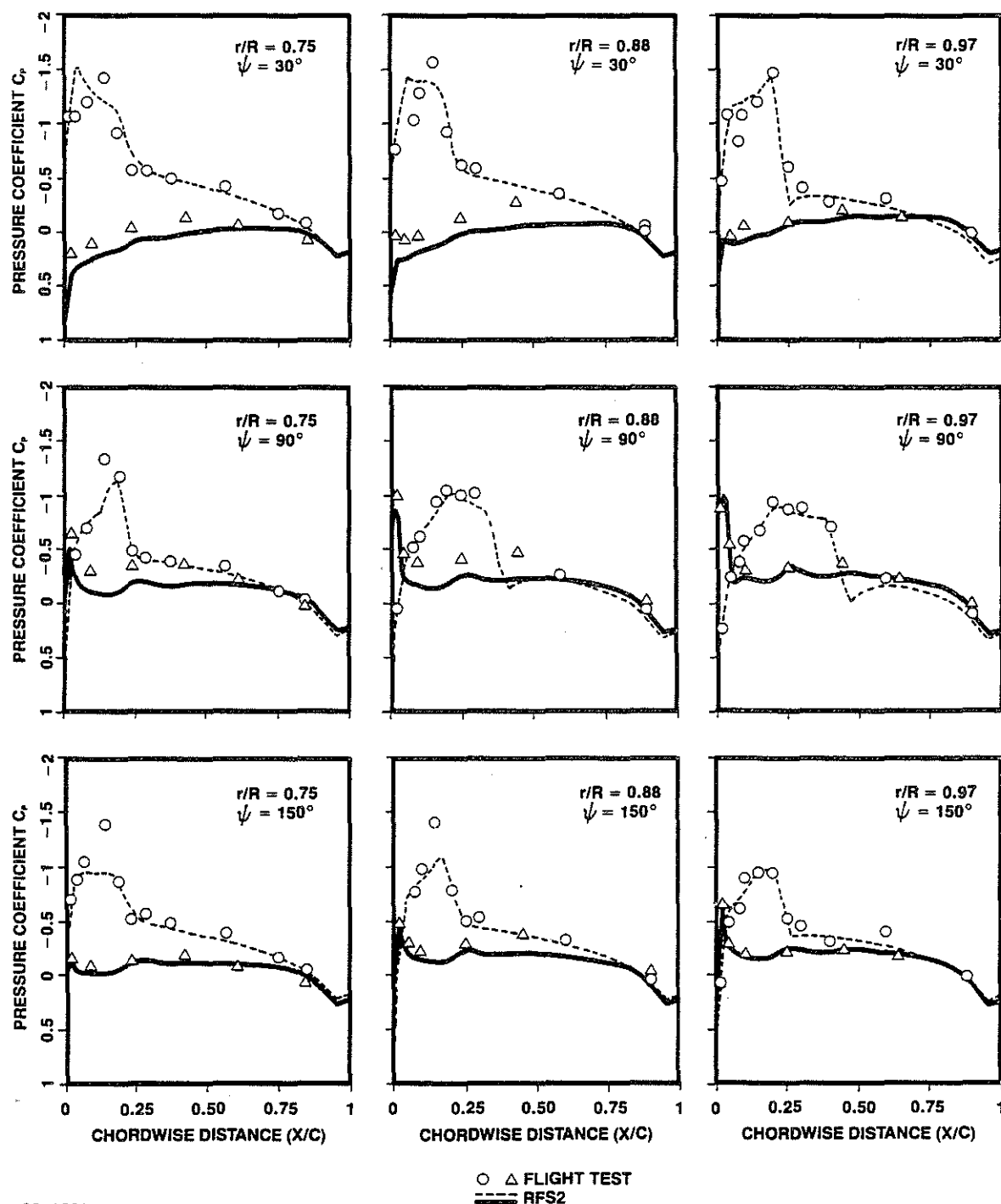
Fig. (1) Comparison of RFS2 predictions and flight test blade surface pressure
data for the three-bladed Aerospatiale Gazelle SA349/2 rotor
(M_t = 0.63, μ = 0.378, CT/σ = 0.0645)

Fig. (1) continued
Comparison of RFS2 predictions and flight test blade surface pressure
data for the three-bladed Aerospatiale Gazelle SA349/2 rotor
($M_t = 0.63, \mu = 0.378$, CT/$\sigma = 0.0645$)
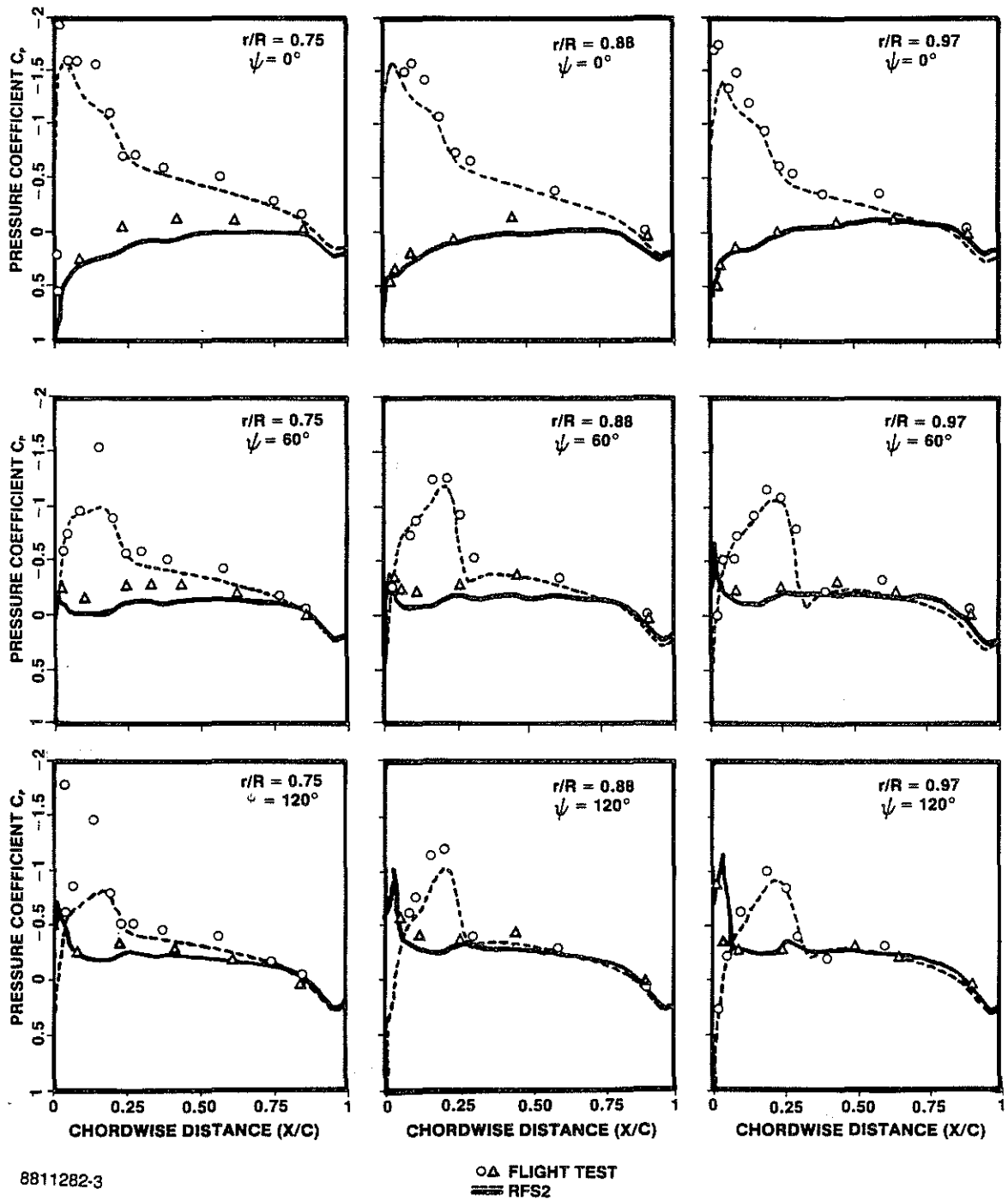
8811282-2

Fig. (2) Comparison of RFS2 predictions and flight test blade surface pressure
data for the three-bladed Aerospatiale Gazelle SA349/2 rotor
$(M_t = 0.63, \mu = 0.344, \ CT/\sigma = 0.0649)$

Fig. (2) continued
Comparison of RFS2 predictions and flight test blade surface pressure
data for the three-bladed Aerospatiale Gazelle SA349/2 rotor
($M_t = 0.63, \mu = 0.344,$ CT/$\sigma = 0.0649$)
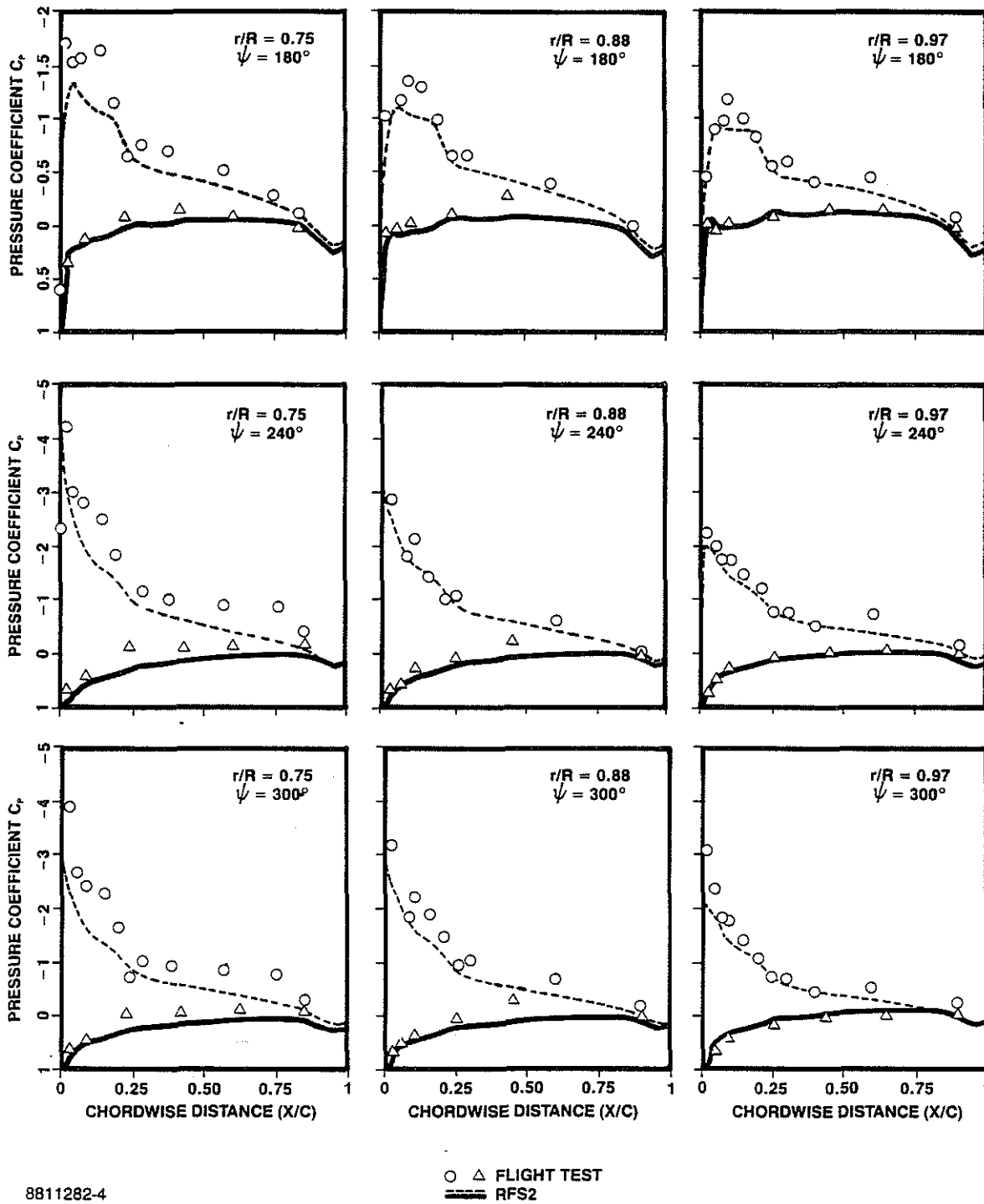
8811282-4

○ △ FLIGHT TEST
═══ RFS2

16-21
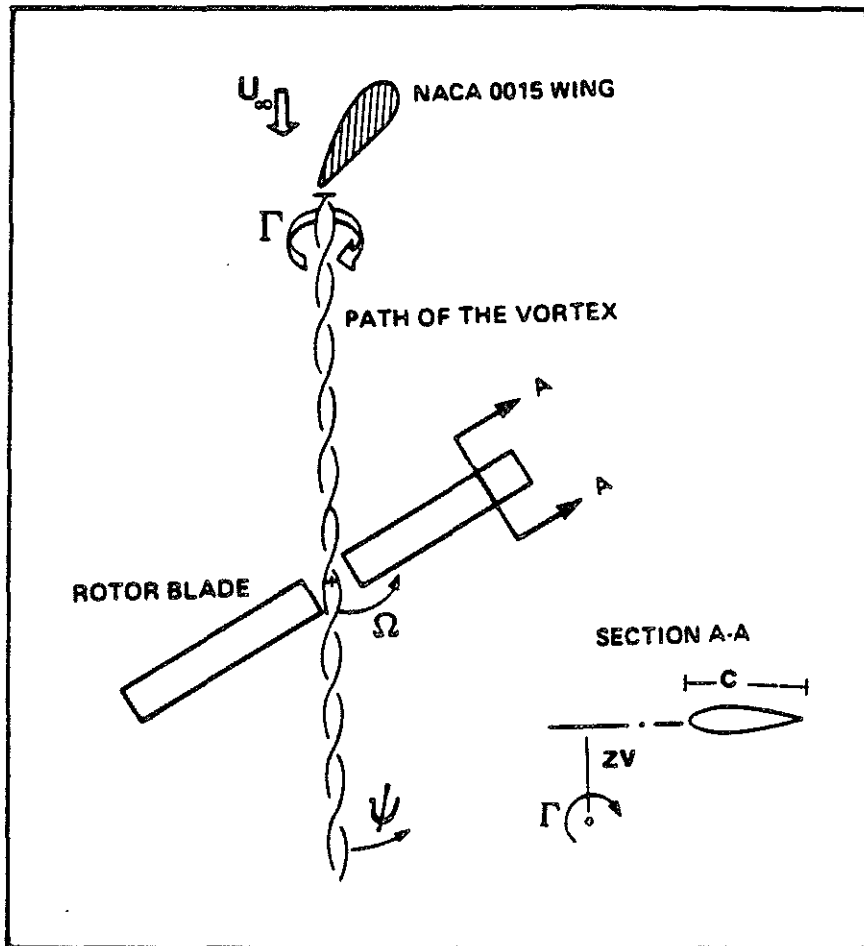
Fig. (3) Sketch illustrating the experimental setup of Refs. [28, 29]
for simulating parallel blade-vortex interactions

(a) ZV/C=0.25
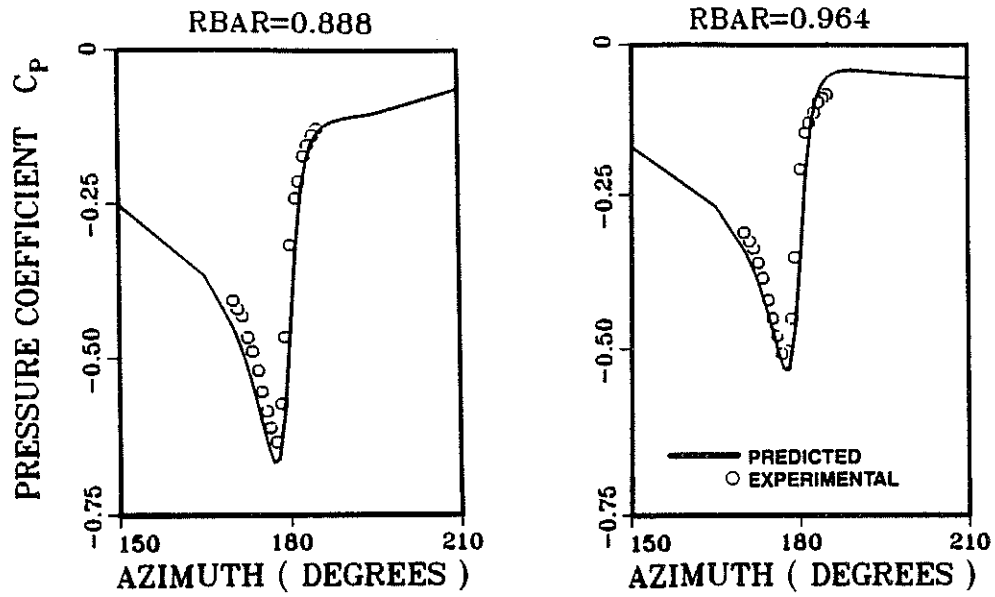
(b) ZV/C=0.40
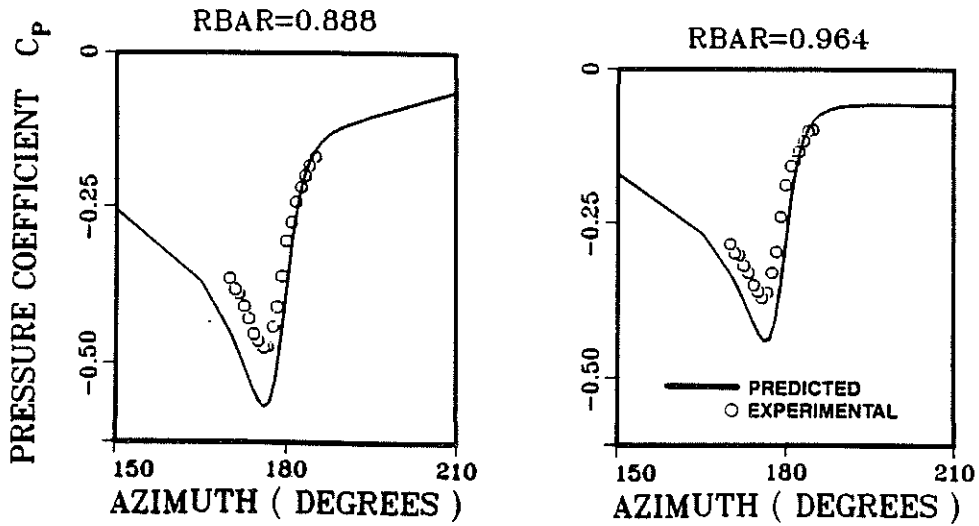
Fig. (4) Predicted and measured upper surface pressures during parallel
blade-vortex interactions
X/C = 0.02, M_{tip} = 0.70, Γ= 0.49, RV/C = 0.225

Fig. (5) Effect of varying the vortex strength on the predicted upper
surface pressure distribution during parallel blade-vortex
interactions
($X/C = 0.02$, Mtip $= 0.70$, $\mu= 0.20$, $ZV/C = 0.40$, $Rv/C =0.225$)
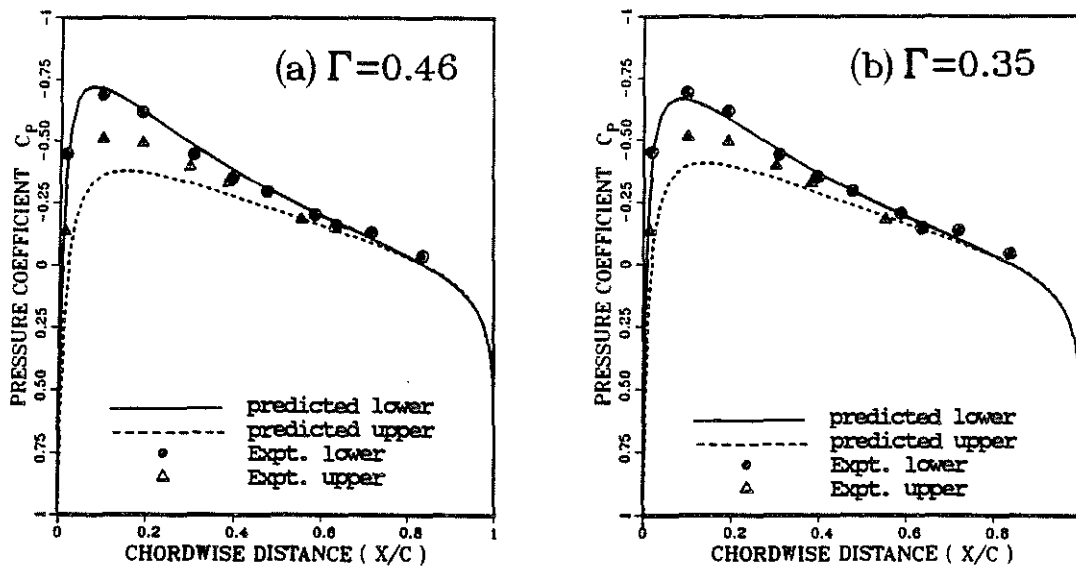
Fig. (6) Effect of varying the vortex strength on the predicted surface
pressure distribution
(Mtip $= 0.60$, $ZV/C = -0.40$, $Rv/C = 0.15$, $\mu=0.20$, Rbar$= 0.888$,
psi $= 178.0$ degrees)
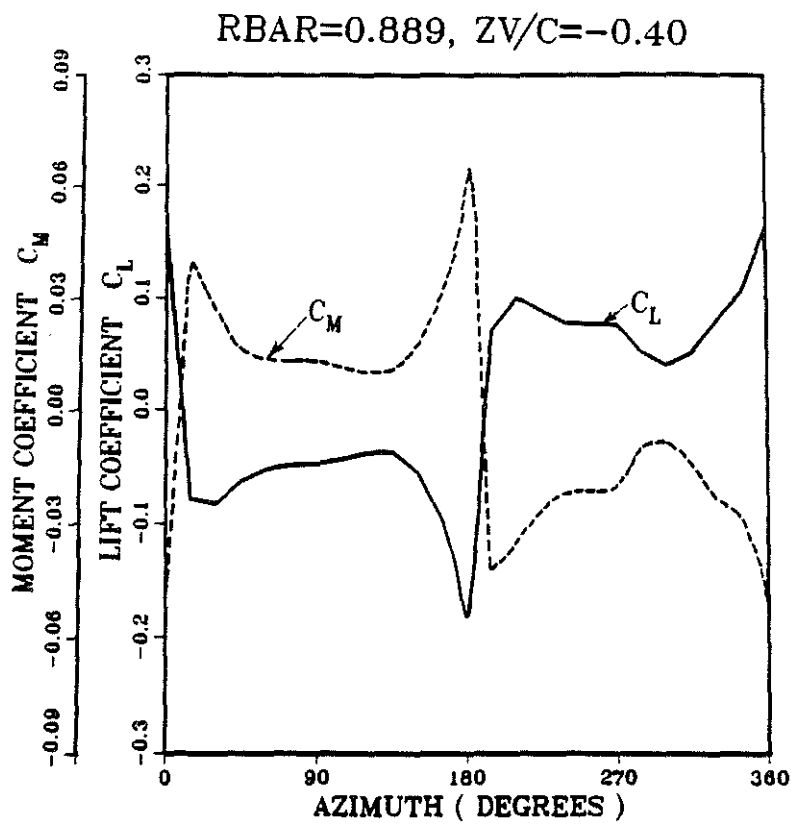
Fig. (7) Predicted sectional lift and moment coefficients during a subcritical parallel blade-vortex interaction
$M_{tip} = 0.60$, $\mu = 0.20$, $\Gamma = 0.46$, RV/C = 0.15

16-25
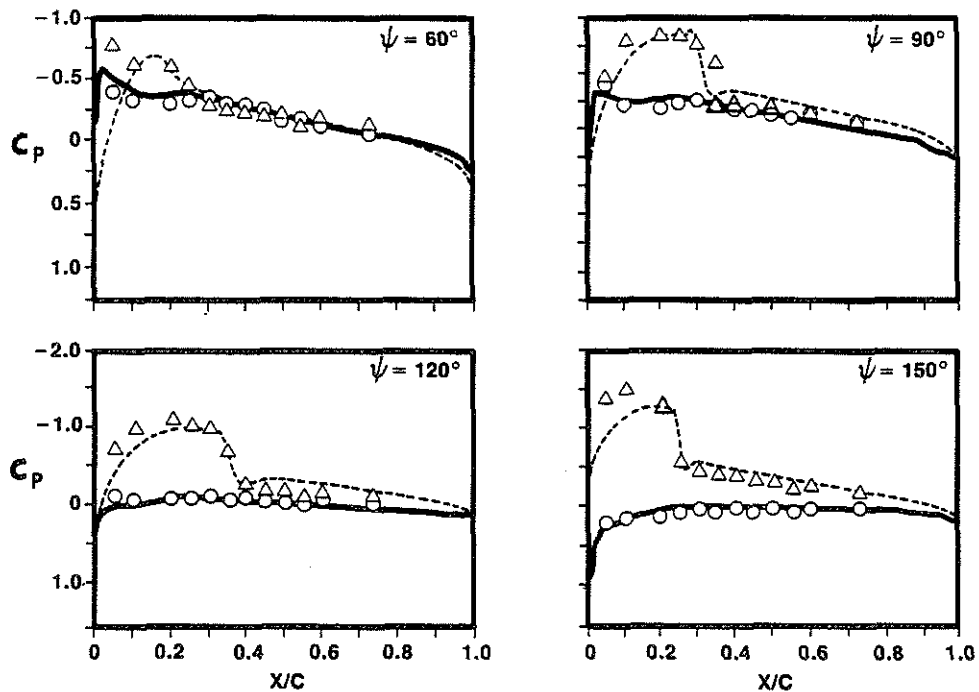
(a) MDROTH EULER PREDICTIONS

△ ○ EXPERIMENT
==== COMPUTED
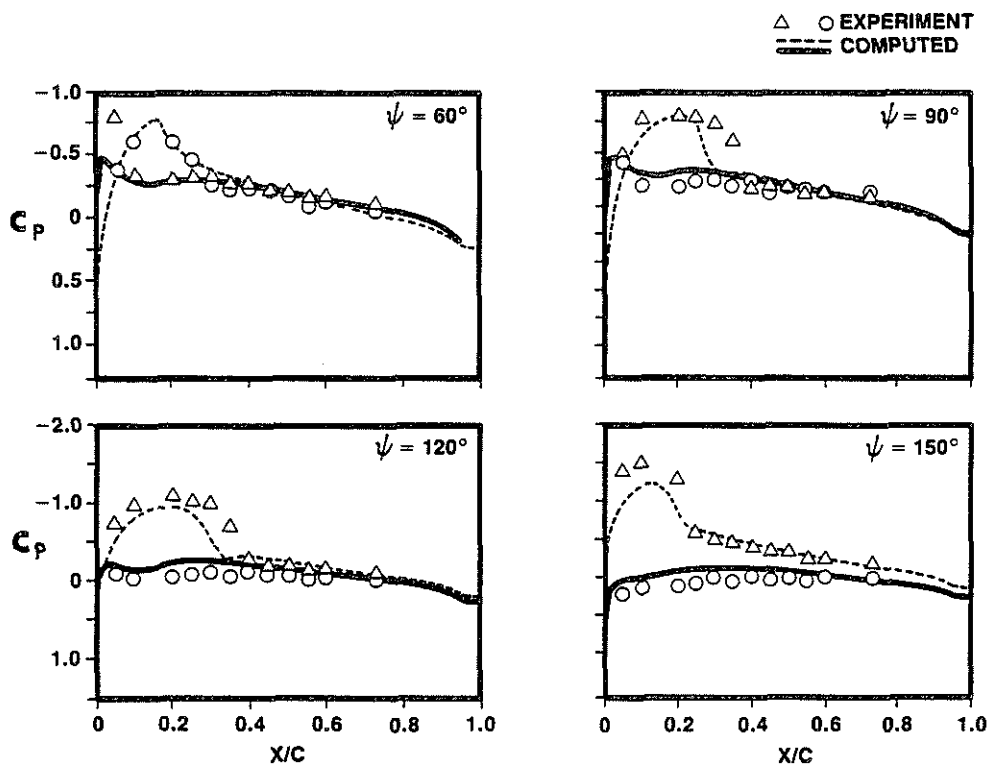
(b) RFS2 FULL-POTENTIAL PREDICTIONS

8811282-5

Fig. (8) Correlations of MDROTH and RFS2 predictions with wind tunnel test data for the ONERA three-bladed rotor
($M_t = 0.629$, $\mu = 0.387$, $C_T/\sigma = 0.0665$, AR = 6.968)
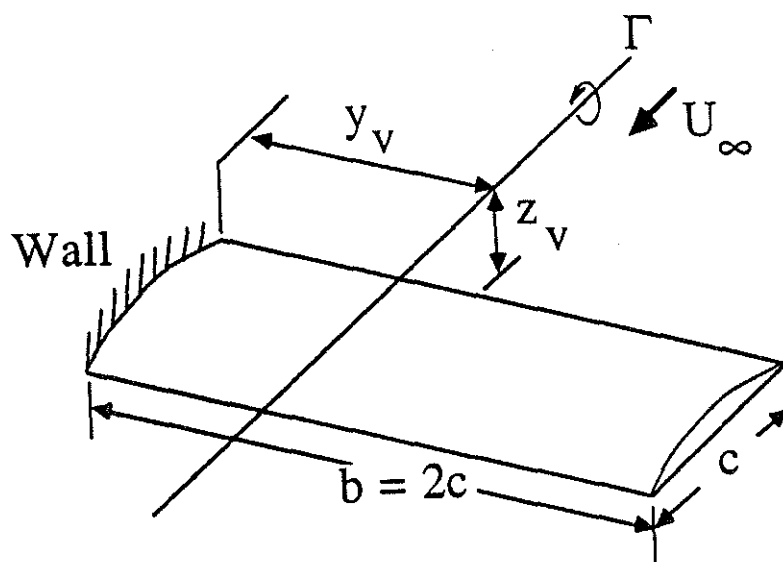
Fig. (9) Sketch illustrating the configuration for blade-vortex interaction
studies using the Euler equations
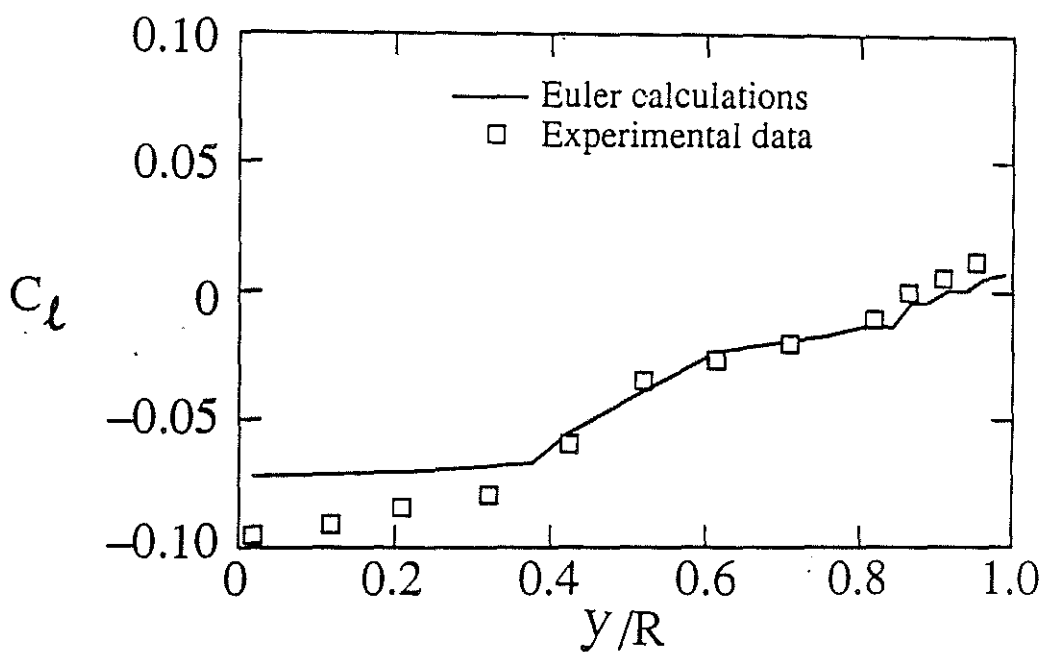
Fig. (10) Predicted and measured spanwise lift distributions during blade-
vortex interaction
(AR = 2, ZV = 1.0, YV = .5, Minf = 2.0, Lamb-vortex Γ= .05, a = .05)
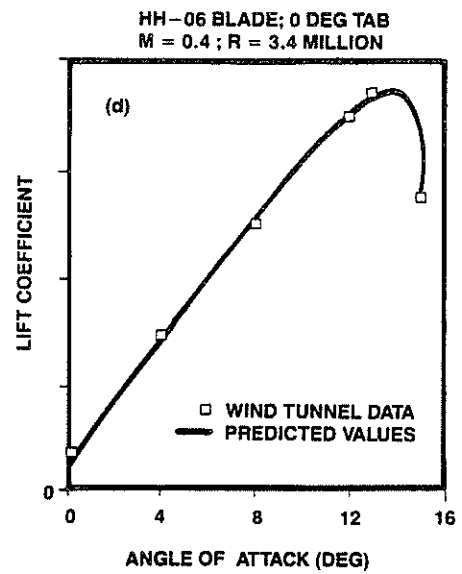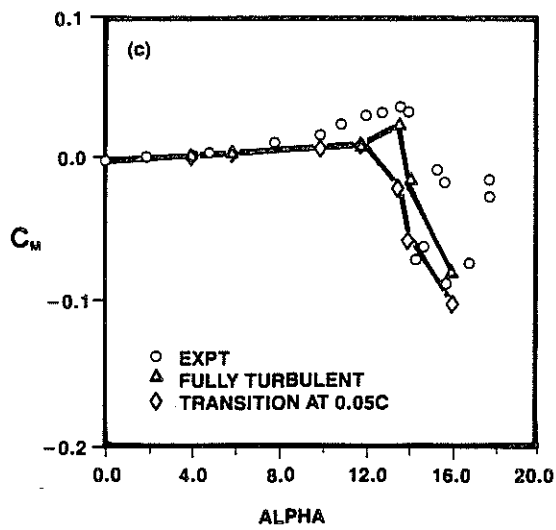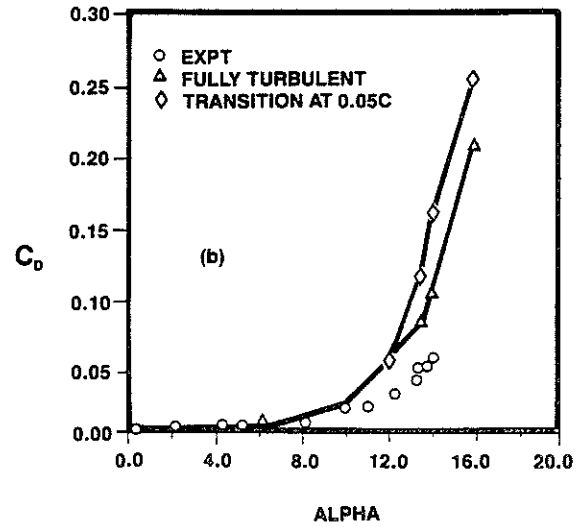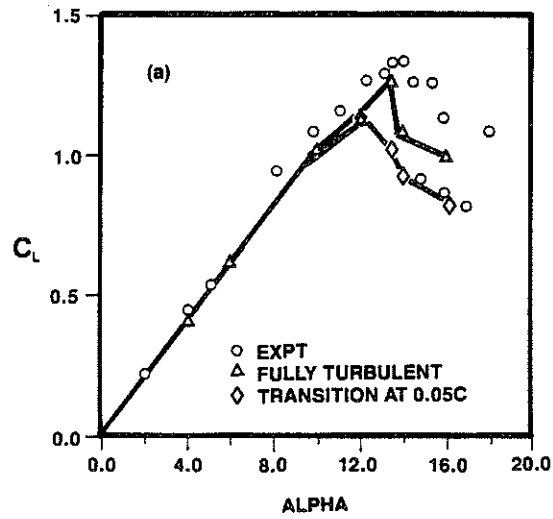
Fig. (11) Computed and measured steady aerodynamic characteristics for the
NACA0012 airfoil (11a-c, $M_t = 0.3$, Re = 3.9 Million) and the
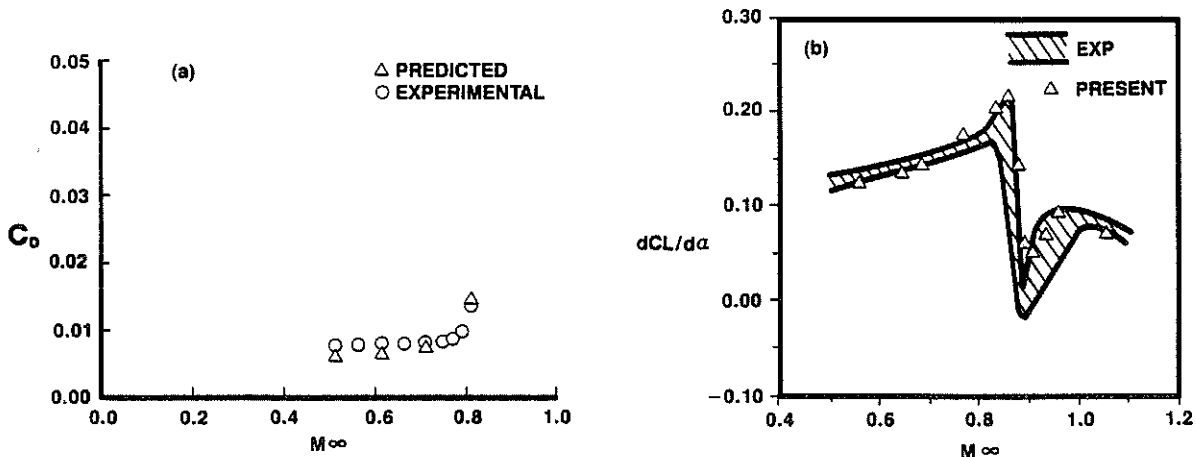HH-06 airfoil (11d, $M_t = 0.4$, Re = 3.4 Million)

8811282-6

Fig. (12) Computed and measured drag and lift characteristics for the
NACA0012 airfoil as a function of free-stream Mach number
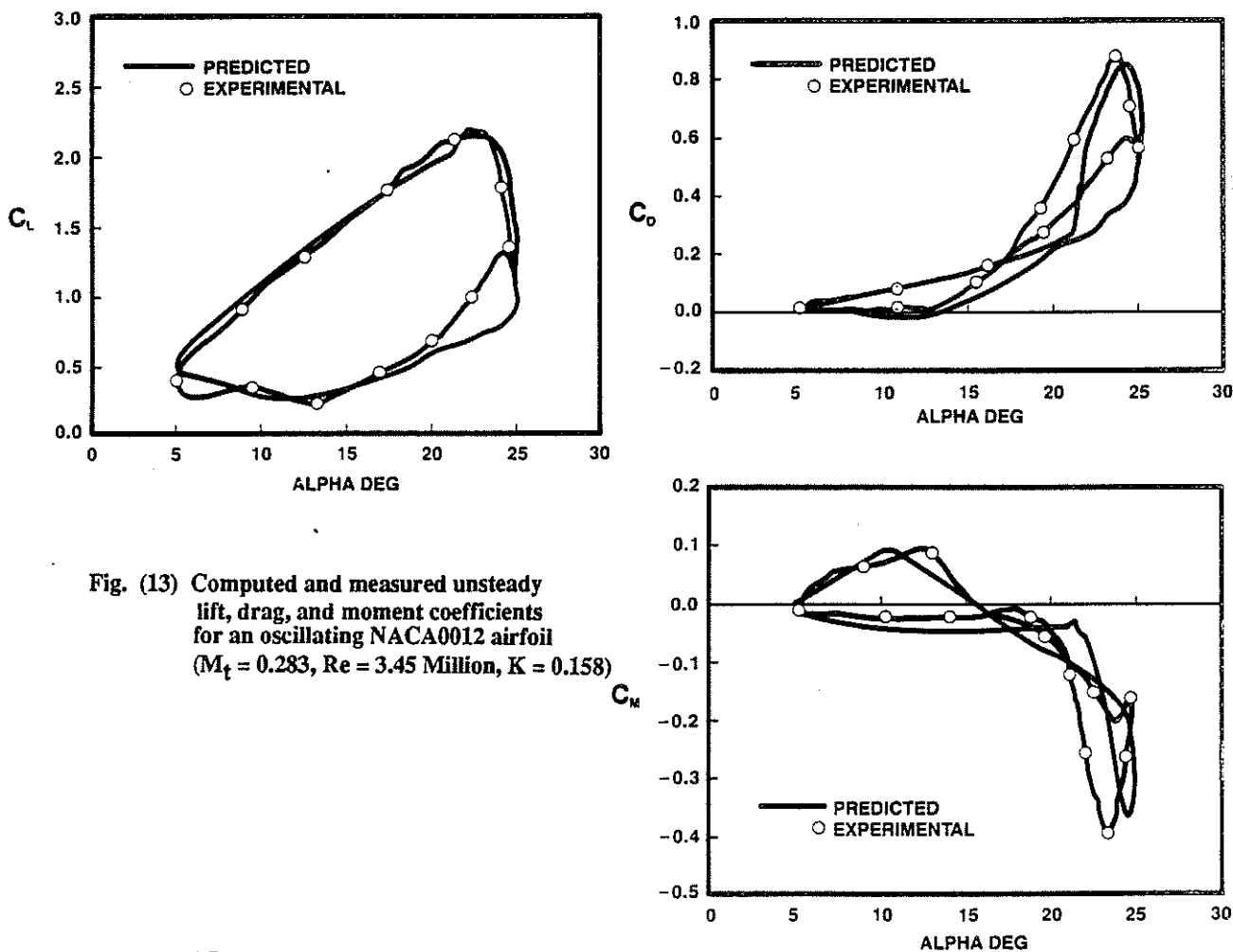(α= 0 deg, Re = 9 million)

Fig. (13) Computed and measured unsteady
lift, drag, and moment coefficients
for an oscillating NACA0012 airfoil
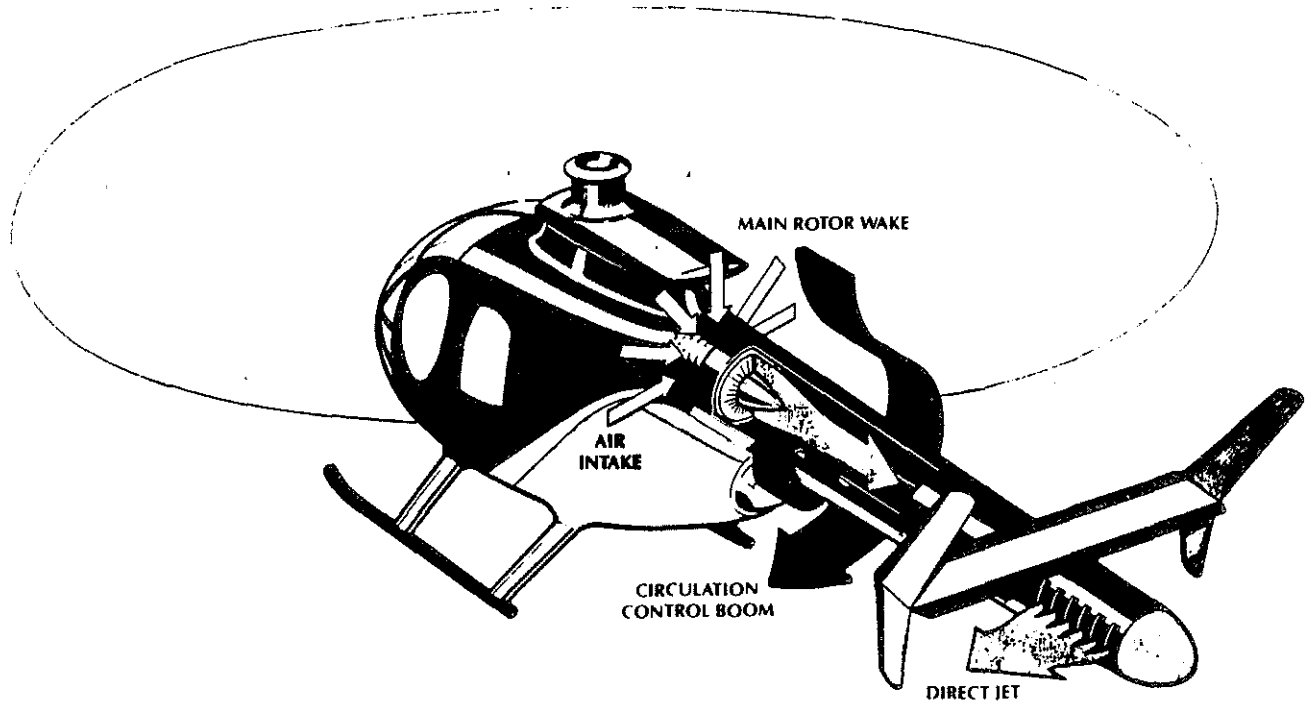(M_t = 0.283, Re = 3.45 Million, K = 0.158)

8811282-7

16-29

Fig. (14) Schematic of the McDonnell Douglas No Tail Rotor (NOTAR) helicopter configuration

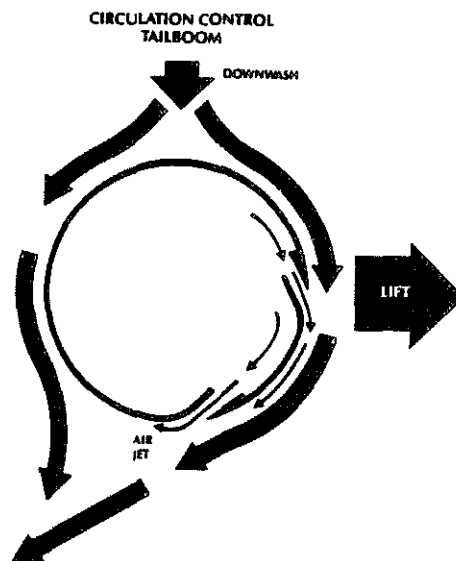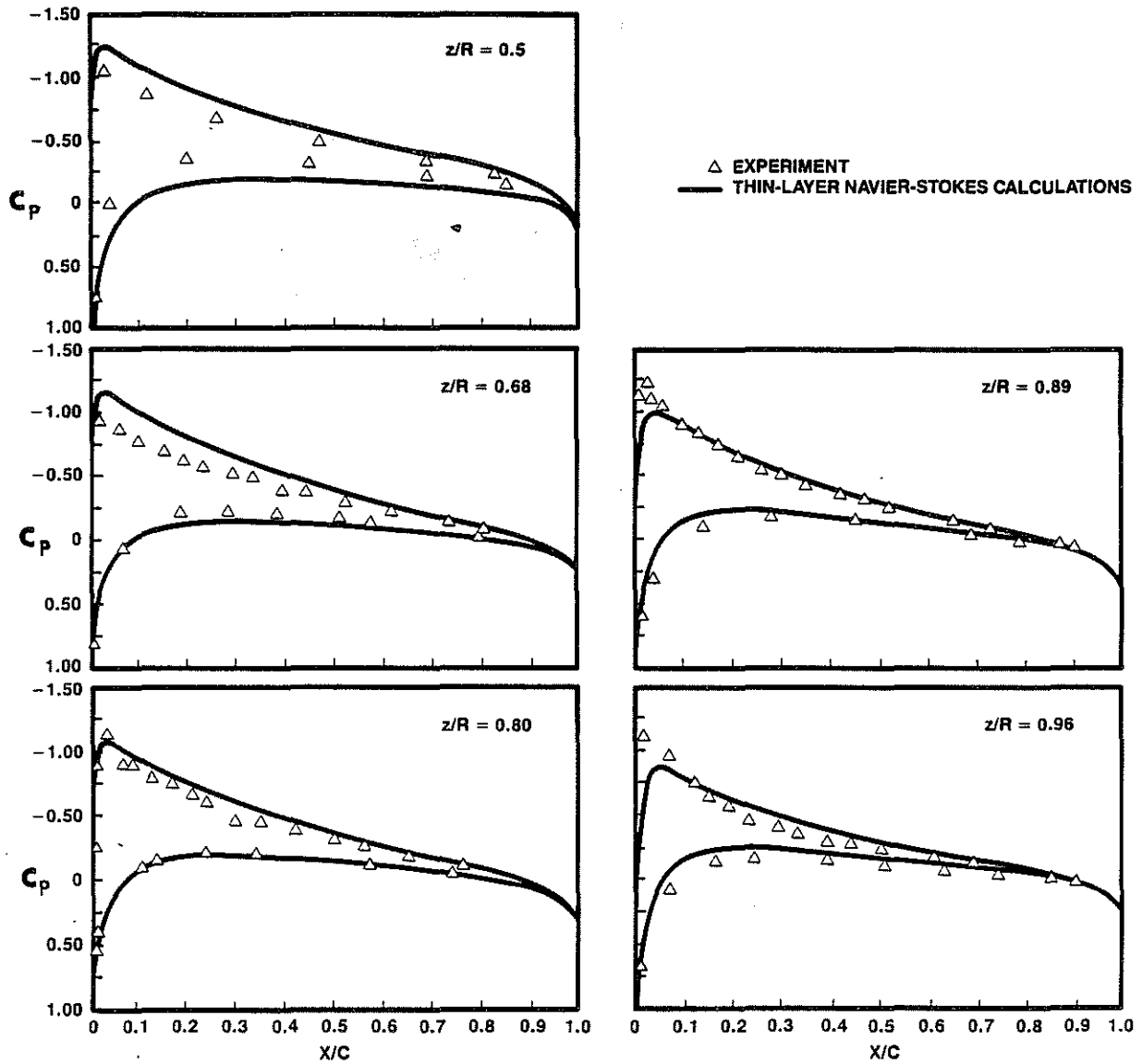Fig. (15) Cross section of a NOTAR circulation control tail boom

Fig. (16) Blade surface pressure distributions on a lifting rotor in hover;
$M_t = 0.612$, $Re_c = 2.67$ Million, $\Theta = 8$, $AR = 6$, untwisted,
rectangular NACA0012 blade

8811282-8

16-31